Characterization of Radiation-Resistant Multimode Optical Fibers for Large-Scale Procurement

Jeremy Blanc, Frank Achten, Antonino Alessi, Adrian Amezcua, Jochen Kuhnhenn, Alain Pastouret, Daniel Ricci, and Iacopo Toccafondo

***Abstract*— This article presents the results of a comprehensive characterization of special radiation-resistant multimode optical fibers, including complementary irradiation tests during mass production. Radiation-induced attenuation measurements were carried out at different wavelengths and the attenuation behavior studied with varying the dose rate. Following a preliminary qualification performed upstream the production, CERN, the European Organization for Nuclear Research, validated the procurement of 500 km of fiber for installation in the accelerator complex and experiments. A strict quality assurance plan, including quality control and irradiation tests, was implemented for monitoring the characteristics of the supplied optical fibers all along the production process. The results show resistance to radiations consistently below 60 dB/km for a total dose of 10 kGy and a dose rate of 0.2 Gy/s and stable optical performance over hundreds of fiber spools produced during a 6-year period.**

***Index Terms*— CERN, optical fiber, procurement process, quality assurance, quality control (QC), radiation effects, radiation-induced attenuation (RIA).**

I. Introduction

MULTIMODE (MM) optical fibers are widely used at CERN (European Organization for Nuclear Research) for control and data transmission. Systems, such as data acquisition for the CERN particle detectors, are regularly consolidated and upgraded using MM optical fibers. The Versatile Link Plus project is, for example, one of those projects, which targets the phase II upgrades of the ATLAS and CMS experiments at CERN [1]. That project requires the development of a radiation-resistant data link, transmitting 5–10-Gb/s data rates in the upstream direction and 2.5-Gb/s rates in the downstream, using MM optical fibers.

Optical fibers are exposed to high-radiation environment in the CERN accelerator complex and experimental areas, where dose rates can reach up to hundreds of kGy per year. This exposure increases the attenuation of the optical fiber, even in the infrared spectral region of interest for optical communications [2]. This phenomenon can lead to such degradations that the concerned systems can no longer operate. The failure of a fiber used in control systems could result, for example, in the interruption of the entire CERN accelerator complex and experiments. The optical fibers installed in those areas must therefore be of a special radiation-resistant type.

In this context, CERN procured 500 km of special radiation-resistant MM optical fiber (RR-MMF). CERN requirements have led to the setting up of a quality assurance plan (QAP) aiming at monitoring the quality level of the supplied RR-MMF and at ensuring the compliance with the CERN requirements. This quality assurance process is described in detail thereafter. Results put in evidence how an early screening, during the production phase, of the performance of the irradiated fibers, allows for a prompt identification of nonconformities and consequent production tuning.

Manuscript received March 6, 2021; revised April 6, 2021; accepted April 8, 2021. Date of publication April 21, 2021; date of current version July 16, 2021.

Jeremy Blanc, Daniel Ricci, and Iacopo Toccafondo are with CERN, European Organization for Nuclear Research, CH-1211 Geneva, Switzerland (e-mail: jeremy.blanc@cern.ch; daniel.ricci@cern.ch; iacopo.toccafondo@cern.ch).

Frank Achten, Adrian Amezcua, and Alain Pastouret are with the Prysmian Group, 5651 CA Eindhoven, The Netherlands (e-mail: frank.achten@prysmiangroup.com; adrian.amezcua@prysmiangroup.com; alain.pastouret@prysmiangroup.com).

Antonino Alessi and Jochen Kuhnhenn are with the Fraunhofer-Institut Naturwissenschaftlich Technische Trendanalysen (INT), D-53879 Euskirchen, Germany (e-mail: antonino.alessi@int.fraunhofer.de; jochen.kuhnhenn@int.fraunhofer.de).

Color versions of one or more figures in this article are available at https://doi.org/10.1109/TNS.2021.3074633.

Digital Object Identifier 10.1109/TNS.2021.3074633

II. Optical Fiber Qualification

The radiation-induced attenuation (RIA) of the optical fiber originates from the formation of color centers in the optical fiber glass when exposed to radiation, and such centers are mainly created by the ionization of atoms in the glass structure [3]. These defects absorb light at different wavelengths depending on their types and can recombine in other defects [4]. Their formation is strongly correlated with the fiber manufacturing process (e.g., dopant and doping level, production process, drawing conditions) [5]–[8] and to the irradiation conditions (e.g., dose rate, total dose, light power, temperature) [9]–[11].

A survey of the commercially available RR-MMF brought CERN to implement a collaboration with one fiber manufacturer in order to precisely qualify and to optimize a novel radiation-resistant fiber. The long-lasting efforts in developing an MM fiber suitable for high radiation environment and room temperature resulted in a procurement contract for CERN. This collaboration, and later the contract, was set up with Prysmian Group and the concerned fiber is commercially named "Super RadHard" Multimode Fiber (SRH-MMF). Tighter specifications regarding RIA were established in addition to the base specifications, by mutual agreement, with CERN bearing the responsibility for testing the RIA of the supplied fibers. This optical fiber is a graded index glass fiber with a 50-μm core and a cladding of 125 μm, both doped with fluorine (F-SiO_2) [12]. The presence of fluorine decreases the number

TABLE I
TYPE TEST RESULTS PERFORMED BY PRYSMIAN ON THE RR-MMF UNDER STANDARD ENVIRONMENTAL CONDITIONS

	Wavelength (nm)	Specifications	Results
Attenuation (dB/km)	850 1300	≤ 3.5 dB/km ≤ 1.0 dB/km	1.796 0.360
Effective group index of refraction	850 1300		1.465 1.461
Bending losses (dB) (2 turns on radius 15 mm)	850 1300	≤ 0.5 dB ≤ 0.5 dB	0.2 0.2
Bending losses (dB) (2 turns on radius 7.5 mm)	850 1300	≤ 1.0 dB ≤ 1.0 dB	0.7 0.8
Zero dispersion wavelength (nm)		$1295 \leq \lambda_0 \leq 1340$	1275
Zero dispersion slope (ps/nm^2.km)	$1295 \leq \lambda_0 \leq 1310$ $1310 \leq \lambda_0 \leq 1340$	≤ 0.105 $\leq 0.000375(1590-\lambda_0)$	0.0998
Rayleigh backscatter coefficient (dB) for 1 ns pulse	850 1300		-67.4 ± 0.4 -74.8 ± 0.4
Tensile strength (GPa)		≥ 3.8	4.45
Average strip force (N)		$1.0 \leq F_{avg} \leq 5.0$	2.0
Peak strip force (N)		$1.0 \leq F_{peak} \leq 8.9$	4.6

of strained bonds [13], [14], increasing the radiation hardness of the silica-based optical fibers [14]–[16].

CERN requirements and the qualification test results of the procured optical fiber are described and discussed in Section II-A. A rigorous qualification of the procured special optical fiber type has been performed in order to ascertain the compliance with CERN requirements, especially in terms of radiation resistance.

A. CERN Requirements

The selected optical fiber type shall be MM and compatible with international standards ITU T G.651.1 and IEC 60793-2-10 for telecom fibers. Any deviation from the standards had to be addressed to CERN during the contract tendering phase.

CERN requested the qualified optical fiber to have an RIA below 60 dB/km for light with a wavelength of 850 $\pm$ 30 nm and below 10 dB/km for light with a wavelength of 1300 $\pm$ 30 nm after an exposure to 10-kGy total ionizing dose (TID) at 25 $\pm$ 3 °C. The RIA shall not exceed the specified limits for light power ranging from 10 up to 25 μW and dose rate ranging from 0.01 up to 0.2 Gy/s. Here, Gy always means Gy(SiO_2).

B. Type Tests

Type tests under standard environmental conditions were asked to the manufacturer in order to demonstrate the conformity of the supply to the CERN requirements. Those tests were performed on representative samples of the production in accordance with IEC 60793.

Table I shows the performed tests and their results. The RR-MMF complies with IEC 60793-2-10 (A1 fiber category) and ITU-T G.651.1, with exception for the chromatic dispersion characteristics. When measured, the zero-dispersion wavelength shows lower value compared to the international standards specifications. This value is attributable to the presence of fluorine instead of germanium, usually used in the core of standard MM fiber. However, a smaller chromatic dispersion coefficient consequently improved the fiber behavior at 850 nm. Hence, the fiber was globally accepted.

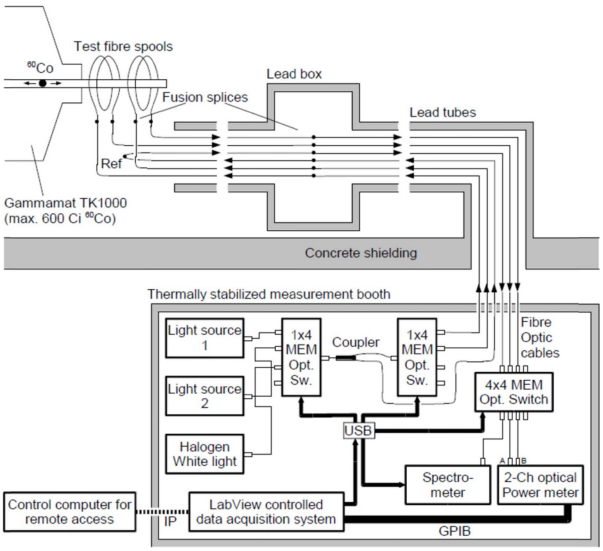

Fig. 1. Schematic of the laboratory irradiation setup in Fraunhofer INT (Euskirchen).

C. Irradiation Test

Although RR-MMF is planned to be installed in mixed radiation fields, irradiation tests were performed with gamma rays in Fraunhofer INT (radiation facilities in Euskirchen, Germany). Several studies investigated the impact of the radiation types on optical fiber and concluded that RIA is mainly dominated by radiolysis and is proportional to the total ionizing dose [10]–[17]. As gamma rays mainly generate damages via the radiolysis effect, that type of source is suitable for our tests.

The irradiation tests were performed according to the setup shown in the schematic of Fig. 1. Two 60-m-long optical fibers were irradiated at the same time, each fiber being coiled around an aluminum spool of defined radius and placed around a ^{60}Co source of known radioactivity. The spool diameter was kept above 110 mm to avoid macrobending influence during the irradiation [18]. The distance of the sample from the source determines the dose rate at which the fiber is exposed to. The two irradiated samples are installed at exactly the same position and therefore irradiated under the same irradiation and environmental conditions.

The experimental setup is designed for irradiation tests at room temperature (25 $\pm$ 3 °C) and consists of two highly stable LED light sources emitting at 830 and 1310 nm and a white light source for spectral attenuation measurement (from 950 to 2000 nm). Precision power meters and a spectrometer, in the case of the spectral analysis, monitor the change in output light power. Transition between samples, light sources, and detectors is done, thanks to optical switches [19]. The setup switches between samples every 10 s for the discrete measurements, and every 100 s a spectral measurement is done in each sample.

Fig. 2 shows the results of the qualification irradiation tests performed on the RR-MMF at four different dose rates (0.02, 0.20, 0.50, and 1.00 Gy/s) up to doses of 2.1, 10, 1000, and 100 kGy, respectively, and at two different wavelengths (830 and 1310 nm) for a light power of -21.5 ± 1.5 dBm.

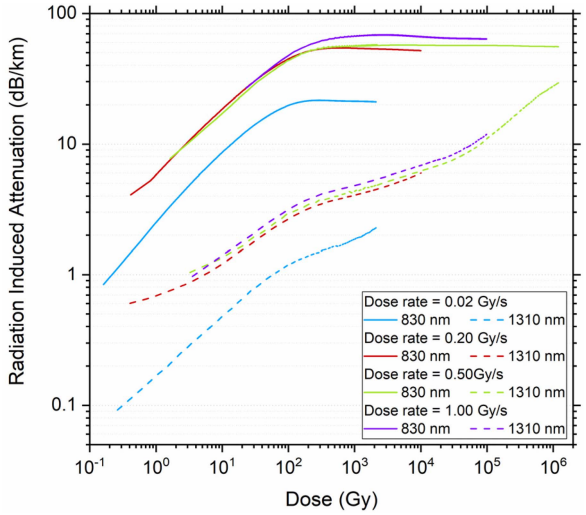

Fig. 2. Irradiation test results of the qualified optical fiber (RR-MMF) at different dose rates.

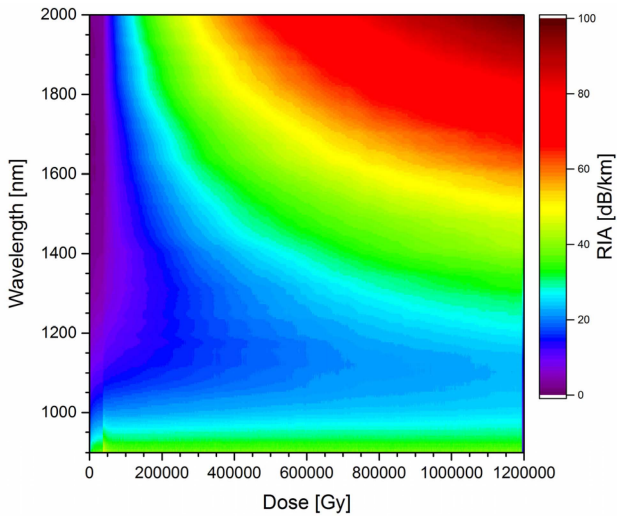

Fig. 3. Evolution of spectral measurement of the RIA for the qualified optical fiber (MM-RRF) at 0.5 Gy/s.

The figure shows that regardless of the dose rate, the RIA at 830 nm increases with the accumulated dose, and then, from a total dose varying from 50 to 250 Gy in the function of the dose rate, saturates, while remaining constant or even decreasing. The variation in dose rate, from 1.0 down to 0.2 Gy/s, does not led to major changes in the RIA, whereas RIA at 0.02 Gy/s is about three times lower. The dose rate dependence of the RIA is attributed to the competition of defects creation and annealing during the exposure [20]. The defects generation rate is lower at low dose rate, while the defects annealing rate is similar at both dose rates, for a given type of defect when all the other parameters like temperature and injected light are fixed. It can be deduced from these results that the defects creation is less affected when the dose rate is changed in the range between 0.02 and 0.2 Gy/s. The RIAs at 1310 nm rapidly increase at the beginning, slow down, and increase rapidly again. This phenomenon is characteristic of the fluorine-doped fibers and is well described in other studies [21], [22].

Fig. 3 shows the spectral measurement of the RIA for the RR-MMF from 900 up to 2000 nm, for a light power of −24 dBm, for a dose rate of 0.5 Gy/s. At short wavelengths, the RIA increases quickly and then it stabilizes to almost constant values. In comparison, the RIA increases continuously with the dose at longest wavelengths. An extraction of the spectral curves at 1, 10, 100, and 1000 kGy is shown in Fig. 4. The wavelength with the lowest RIA decreases from 1700 nm at 1 kGy down to 1100 nm at 1 MGy. It is apparent from these curves that the attenuation measured at low dose is mostly affected by the tail of the RIA at low wavelength and then at higher dose by the tail of RIA at high wavelength. This double contribution explains the RIA kinetics, with an increase, followed by a saturation and then followed again by a second increase.

Fig. 5 shows the annealing behavior of the qualified optical fiber at the four different dose rates and at both 830- and 1310-nm wavelength. The annealing occurs when the irradiation stops and presents a fast decrease of the RIA at the beginning. The faster annealing at 830 nm is observed

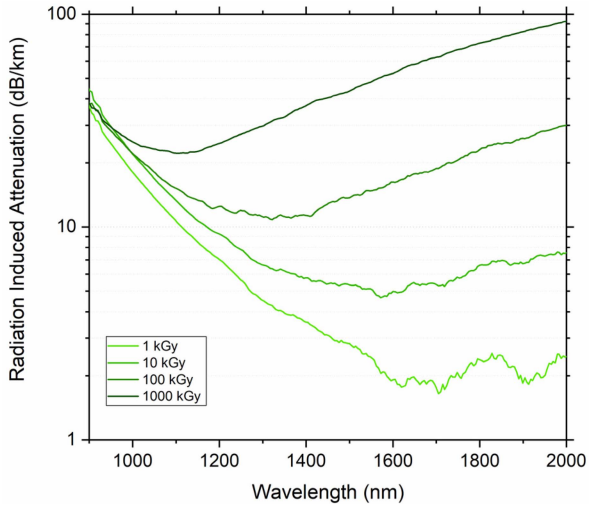

Fig. 4. Spectral measurement of the RIA for the qualified optical fiber (MM-RRF) at different total integrated dose and for a dose rate of 0.5 Gy/s.

for irradiation test performed at 1.0 Gy/s and the slower at 0.02 Gy/s.

The annealing of the fibers varies between 58% and 86% at 830 nm and between 17% and 68% at 1310 nm. Despite the important annealing, it is well known that the RIA would return promptly to its previous level as soon as the optical fiber is exposed again to radiation [25].

During the qualification of the RR-MMF under radiation, rapid and periodic changes of RIA were noticed during the attenuation measurement. Those changes of RIA revealed to be linked to the switching of the light sources and therefore to the change of light wavelength and power. This effect is well known and is called photobleaching effects. For the interpretation of the results, these variations were negligible and therefore the curves were smoothed in the graphs. Further investigations have shown a strong dependence of the RIA on the transmitted light power at specific wavelengths. The results of these investigations are documented in another paper [26].

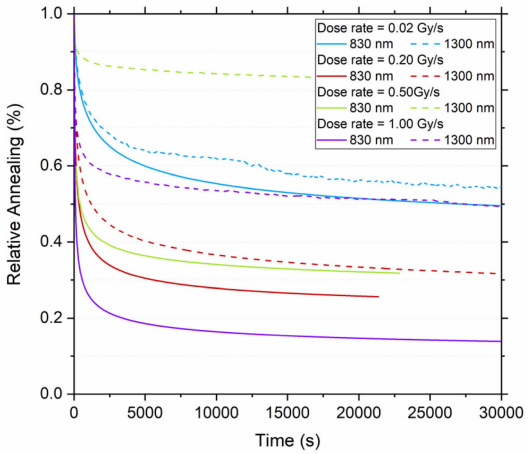

Fig. 5. Relative annealing of the qualified optical fiber (RR-MMF) at different dose rates.

III. Production

The qualified fiber showing performance in line with the CERN requirement, a contract was initially signed for a period of 2 years. The production process, quality control (QC), and irradiation tests are described in this section.

A. Process

The qualified RR-MMF is produced at Prysmian Group's optical fiber manufacturing facility in Eindhoven, The Netherlands. Thin layers of glass are successively deposited inside a quartz tube using a plasma chemical vapor deposition (PCVD) process [27], [28]. The energy generated by the plasma is precisely concentrated inside the tube, allowing the deposition of thousands of thin layers, leading to a great control of the refractive index. During this step, both the fiber core and the cladding are created.

Silicon tetrachloride ($SiCl_4$) is the gas compound used to produce high-purity silicon dioxide (SiO_2), also known as silica, during the PCVD process. The volume of chlorine (Cl) shall be well controlled as it acts as a precursor for the generation of Cl_0 and Cl_2^- absorbing defects [4]–[29]. The concentration of these defects varies with the irradiation parameters and is strongly correlated with the presence of fluorine [8], which is the only dopant of the fiber discussed in this article. The fluorine is introduced through the silicon tetrafluoride (SiF_4) compound [30], which, used in large excess, can degrade the deposition of layers from the gas phase.

In addition to enhancing the radiation resistance of the fiber, the use of fluorine allows reducing the refractive index and consequently to manufacture a graded index fiber [12]. The profile of the refractive index directly impacts the bandwidth of the fiber.

The chemical vapor composition shall therefore be accurately set to reach the best performances.

The drawing is performed at low speed to minimize the quantities of defects created in the glass network. A dual-layer coating system is applied on the fiber during its drawing. The optimized coating system reduces the stress applied to the cladding while keeping a good mechanical protection.

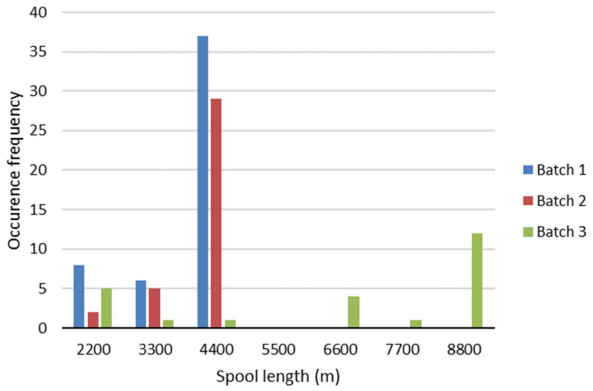

Fig. 6. Number of delivered RR-MMF individual lengths.

B. Schedule and Quantities

The 500 km of RR-MMF ordered by CERN were divided in three batches, produced upon request. An initial order of 200 km was issued in December 2014, followed by a second of 150 km in August 2015 and a third order of 150 km in October 2018.

The standard lengths available at the beginning of the contract were 2200, 3300, and 4400 m. Thanks to process improvement, Prysmian was able to supply spools with a length up to 8800 m for the third batch. Each spool is identified by a unique ID, including the preform number. In total, 111 spools, originating from 29 preforms, have been delivered. The repartition of the individual fiber lengths is shown in Fig. 6. Among the delivered spools, 24% were shorter than 4400 m, 60% were 4400-m long, and 16% were longer than this length.

C. Manufacturer QC

In the frame of this contract, several QC tests were requested to the manufacturer in order to assess the performance of the delivered fiber and its compliance with both the international standards and the CERN requirements. These QC tests include optical tests [i.e., attenuation, overfilled modal bandwidth (OMB), bending losses, numerical aperture], dimensional tests (e.g., core/cladding/coating diameters, noncircularity, concentric error), and mechanical tests (e.g., proof stress). Some of those tests were requested per preform and others per individual fiber length.

The threshold implemented by Prysmian for the optical fiber attenuation is more restrictive in regard to the standards requirements. This allows a better monitoring of the fiber quality after being drawn. The implemented thresholds are 2.5 dB/km at 850 nm and 0.5 dB/km at 1300 nm against 3.5 and 1.0 dB/km, respectively, in the international standards. An overview of the measured attenuation is given in Fig. 7. The measured attenuation of each fiber is shown with a blue solid line for 850-nm wavelength and with a red solid line for 1300 nm. The dashed lines represent the acceptance thresholds for those two wavelengths. Average values of 1.88 and 0.42 dB/km were observed at 850 and 1300 nm, respectively. It can be noticed that attenuation is quite constant among the delivered fibers, with a standard deviation of about 0.046 dB/km at both wavelengths.

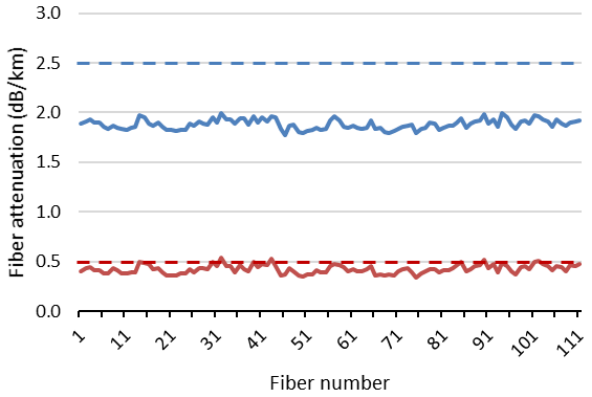

Fig. 7. Fiber attenuation of all delivered fibers at 850 nm (blue solid line) and 1300 nm (red solid line). Dashed lines: attenuation threshold values implemented by Prysmian.

In addition to the attenuation measurement, a spectral analysis was requested for each preform. Fig. 8 presents the spectral measurement of the pristine attenuation measured for each sample, for a wavelength from 450 up to 1700 nm, using the cut-back method in accordance with IEC 60793-1-40. In fact, the spectral measurement could not be conducted for the full range of wavelengths and had to be performed in two times: from 450 to 800 nm using a 400-m sample and from 600 to 1700 nm using a fiber spool. The vertical dashed lines correspond to the main telecom wavelengths for MM fiber (850 and 1300 nm).

The curves present four main attenuation peaks at 630, 1270, 1383, and 1530 nm. The first peak at 630 nm is generally attributed to the presence of nonbonding oxygen hole center (NBOHC) in the glass. This peak, called "drawing peak" by the manufacturer, is influenced by the drawing conditions (such as tension and speed) and the glass composition. The attenuation increase at 1270 nm is largely assimilated to the presence of interstitial O_2 molecules trapped into the glass [23]. This explanation mainly comes from luminescence experiments. Since the beginning of silica optical fiber development, the loss peak centered around 1383 nm was recognized as the absorption of the hydroxyl group (OH). This peak, called "Water peak," causes increased attenuation from about 1360 to 1460 nm.

The last peak, located at about 1530 nm, is the signature of Si–H bonds in glass [4]–[24]. This defect is mostly observed in silica or fluorosilicate glass matrices. These last three peaks are highly sensitive to the presence of water molecules in the fiber environment.

By comparing the three delivered batches, we noticed, in the second batch, a great reduction of the attenuation peaks located at 1383 and 1530 nm. As mentioned above, those peaks are mainly influenced by the environmental conditions such as the presence of humidity, but also by the production tolerances and the samples measurement conditions, such as the fiber tension.

Table II presents the other optical tests performed by the manufacturer in order to ensure the compliance of the RR-MMF with the international standards. Both the test results and the required values are presented. The thresholds implemented for the bending losses are set by Prysmian below the international standards, 0.5 dB against 1.0 dB at both wavelengths.

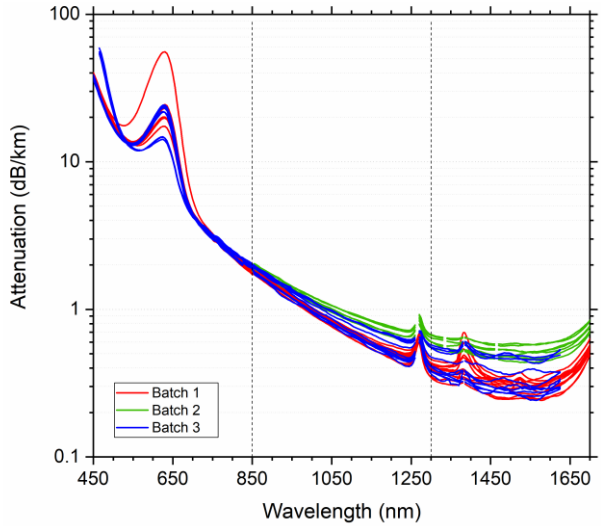

Fig. 8. Spectral measurement of the pristine radiation-resistant fiber attenuation.

TABLE II
OPTICAL TEST RESULTS FROM THE RR-MMF MANUFACTURER

	Specification	Mean	Min.	Max.	Standard deviation
Bending losses (dB) @ 850 nm (2 turns around 15 mm radius)	< 0.5	0.274	0.09	0.47	0.0876
Bending losses (dB) @ 1300 nm (2 turns around 15 mm radius)	< 0.5	0.302	0.10	0.57	0.1102
Overfilled Bandwidth (MHz.km) @ 850 nm	≥ 500	1283	521	7654	959
Overfilled Bandwidth (MHz.km) @ 1300 nm	≥ 500	1109	563	2385	424
Numerical Aperture	0.200 ± 0.015	0.200	0.186	0.213	0.005

Dimensional tests were performed on each RR-MMF delivered, with a proof test value of 0.7 GN/m^2. Fig. 9 presents the dimensional measurement results of the core, the cladding, and the coating diameters of all delivered fibers. A nonconformity at the core level could strongly impact the mode distribution, as well as a nonconformity at the cladding level can prevent the fitting of the fiber in a connector ferrule. These are only two examples that highlight the importance of rigorously monitoring the geometrical parameters of the produced fibers. Table III gives the parameter specifications and some statistics of the measured values.

D. Irradiation Tests

QC irradiation tests were performed with the setup shown in Fig. 1 by Fraunhofer INT. In order to ensure the compliance of each preform with CERN requirements, the fiber attenuation during and after irradiation needs to be assessed. To do this, the delivery of a 400-m sample for each produced preform was stipulated in the contract. Although only 60 m was required to assess the fiber RIA at the chosen dose rate and optical power, the delivery of a longer sample gave the possibility to perform multiple tests on the same fiber in order to check the reproducibility of the tests or the possible changes in the fiber performance over time.

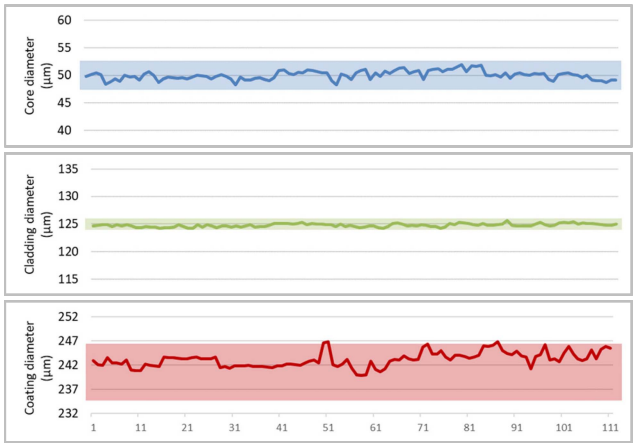

Fig. 9. Geometrical measurement of the core/cladding/coating diameters of all delivered fibers. Colored stripes: dimensional acceptance ranges.

To ensure a reliable comparison of the tests results, the irradiation parameters were fixed at the beginning of the contract. All irradiation tests were performed with a dose rate of 0.2 Gy/s and reached a total accumulated dose of 10 kGy. The light power was kept at -20 ± 1.5 dBm and the temperature at 25 ± 3 °C.

In total, 29 preform samples were irradiated. The irradiation test results of all produced preforms at 830 and 1310 nm are shown in Fig. 10, each curve corresponding to one preform sample and one wavelength. The black dashed lines show the RIA limits specified in the contract for each wavelength. As can be observed from Fig. 10, three samples did not fulfill CERN's requirements as specified in the contract because their RIA was significantly above the limits. In particular, at 830 nm, their RIA was measured to be about a factor 3.5–4 higher than the conform samples. Similarly, at 1310 nm, two of those samples also presented a nonconform RIA about 2–3 times higher than the conform samples at the term of the irradiation, that is, at 10 kGy.

The cause of this nonconformity was investigated by the manufacturer and diagnosed as merely related to machine settings during production. The replacement samples provided after solving the issue showed a behavior conforming with the requirements.

E. Additional Test

The concerned RR-MMF is defined by the manufacturer as a fiber of grade OM2 (determined by ISO 11801), meaning a modal bandwidth of 500 MHz·km. This grade of MM fiber easily supports applications from Ethernet 10 Mbit/s to Gigabit Ethernet (1 Gbit/s) up to 550 m for the latter. However, a fiber of this grade does not provide sufficient bandwidth to support applications at higher transmission speed and are limited to very short link length (e.g., 82 m in the case of 10 Gbit/s Ethernet). In order to reach higher transmission speed, laser sources must be used instead of LED, leading to the development of new methods for qualifying the fiber bandwidth. Differential mode delay (DMD) is one of these methods [31], [32]. Short laser pulses are launched in different positions of the fiber core, by moving the position of the source by small steps across the entire fiber core. The output pluses are monitored in function of time for each launched pulse. The effective modal bandwidth (EMB) is then calculated using time positions and shapes of all pulses and matches them against standardized weight functions that are intended to represent the possible radial launch power distributions of vertical-cavity surface-emitting laser (VCSEL).

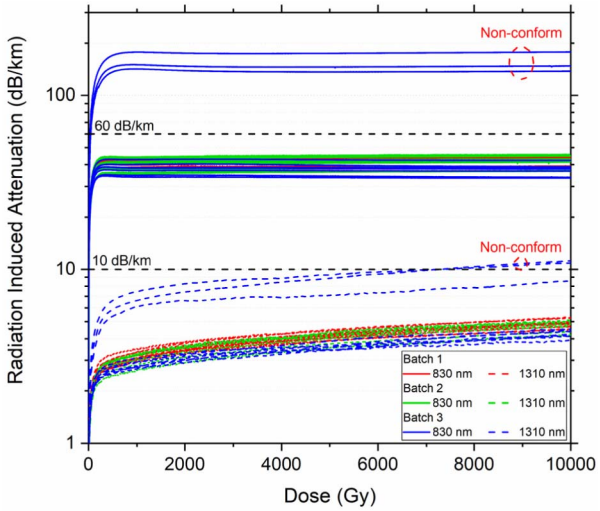

Fig. 10. Irradiation test results of all supplied RR-MMF batches at 850 and 1310 nm.

TABLE III
GEOMETRICAL TEST RESULTS FROM THE RR-MMF MANUFACTURER

	Specification	Mean	Min.	Max.	Standard deviation
Core diameter (µm)	50.0 ± 2.5	50.0	48.3	52.0	0.78
Core non-circularity (%)	< 6.00	1.40	0.25	3.50	0.71
Cladding diameter (µm)	125.0 ± 1.0	124.8	124.2	125.7	0.29
Cladding non-circularity (%)	< 1.0	0.2	0.0	0.6	0.10
Core-cladding concentricity (%)	< 1.5	0.3	0.0	0.8	0.15
Coating diameter (µm)	242 ± 5	243.1	239.9	246.9	1.54
Coating non-circularity (%)		0.6	0.1	1.8	0.34
Coating-cladding concentricity (%)	< 12.5	2.4	0.3	9.2	1.90

TABLE IV
DMD TEST RESULTS FROM THE RR-MMF MANUFACTURER

	OMB at 850 nm (MHz.km)	EMB at 850 nm (MHz.km)
Fibre 1	2919	3344
Fibre 2	5046	3226
Fibre 3	7654	4212
Fibre 4	4895	2179

In the frame of the procurement contract, only the OMB had to be measured through the QC process. However, in order to assess the EMB of the RR-MMF, DMD tests were performed on four of the supplied fiber. The test results are given in Table IV.

For three of the four fibers, these results reveal that the tested fibers could, in fact, be considered as grade OM3. A DMD test would have to be performed on each fiber in order to determine if this one could be considered with a higher grade than OM2.

IV. Conclusion

The QAP put in place in the framework of the large-scale procurement of MM radiation-resistant optical fibers, ensured an accurate follow-up of the production and the compliance of all the delivered fibers with both international standards and CERN requirements.

The irradiation QC tests of the 29 produced batches (i.e., preforms) led to the rejection of 8% of the total MM-RRF supplied, based on the contract specifications. An early detection of the RIA nonconformity was assured by specific irradiation tests implemented by CERN on each preform.

Thanks to the screening performed during the production phase and following the detection of the RIA nonconformity, the production process was tuned during the procurement of the third batch in order to fulfill CERN requirements.

These results put in evidence the importance of the implementation of a strong QAP, especially for such special fibers which are intended to be installed in a high-radiation environment where access to personnel is generally restrained and limited.

References

[1] M. A. Shoaie, D. Ricci, J. Blanc, and S. Machado, "Fibre optics cabling design for LHC detectors upgrade using variable radiation induced attenuation model," *PoS*, vol. 313, pp. 91–95, Mar. 2018, doi: 10.22323/1.313.0091.

[2] E. J. Friebele and D. L. Griscom, "Color centers in glass optical fiber waveguides," in *Proc. Mat. Res. Soc. Symp.*, vol. 61, 1985, pp. 319–331, doi: 10.1557/PROC-61-319.

[3] S. Girard *et al.*, "Overview of radiation induced point defects in silica-based optical fibers," *Rev. Phys.*, vol. 4, Nov. 2019, Art no. 100032, doi: 10.1016/j.revip.2019.100032.

[4] D. L. Griscom, "Optical properties and structure of defects in silica glass," *J. Ceram. Soc. Jpn.*, vol. 99, no. 1154, pp. 923–942, 1991, doi: 10.2109/jcersj.99.923.

[5] Y. Hibino, H. Hanafusa, K. Ema, and S. Hyodo, "Raman study on silica optical fibers subjected to high tensile stress," *Appl. Phys. Lett.*, vol. 47, no. 8, pp. 812–814, Oct. 1985, doi: 10.1063/1.95992.

[6] H. Hanafusa, Y. Hibino, and F. Yamamoto, "Formation mechanism of drawing-induced E' centers in silica optical fibers," *J. Appl. Phys.*, vol. 58, no. 3, pp. 1356–1361, Aug. 1985, doi: 10.1063/1.336107.

[7] E. J. Friebele *et al.*, "Correlation of single-mode fiber radiation response and fabrication parameters," *Appl. Opt.*, vol. 30, no. 15, pp. 1944–1957, May 1991, doi: 10.1364/AO.30.001944.

[8] A. Alessi *et al.*, "Influence of the manufacturing process on the radiation sensitivity of fluorine-doped silica-based optical fibers," *IEEE Trans. Nucl. Sci.*, vol. 59, no. 4, pp. 760–766, Aug. 2012, doi: 10.1109/TNS.2012.2184554.

[9] A. Presland, T. Wijnands, L. D. Jonge, and T. Sugito, "Gamma-ray induced optical absorption in Ge and P-doped fibres at the LHC," in *Proc. 8th Eur. Conf. Radiat. Effects Compon. Syst.*, Cap d'Agde, France, Sep. 2005, pp. PA1-1–PA1-5, doi: 10.1109/RADECS.2005.4365555.

[10] D. L. Griscom, M. E. Gingerich, and E. J. Friebele, "Model for the dose, dose-rate and temperature dependence of radiation-induced loss in optical fibers," *IEEE Trans. Nucl. Sci.*, vol. 41, no. 3, pp. 523–527, Jun. 1994, doi: 10.1109/23.299793.

[11] H. Henschel, J. Kuhnhenn, and U. Weinand, "Radiation hard optical fibers," in *OFC/NFOEC Tech. Dig. Opt. Fiber Commun. Conf.*, Anaheim, CA, USA, Mar. 2005, p. 4, paper OThI1, doi: 10.1109/OFC.2005.192948.

[12] B. G. Risch, B. Overton, J. Rosko, A. Bergonzo, G. Kuyt, and G. Mélin, "Optical fiber and cable reliability for high radiation environments," in *Proc. 61st Int. Wire Cable Symp. (IWCS)*, vol. 61, Dec. 2012, pp. 543–551.

[13] H. Hosono, T. Ogawa, L. Skuja, and M. Mizuguchi, "Fluorine-doped SiO_2 glasses for F_2 excimer laser optics: Fluorine content and color-center formation," *Opt. Lett.*, vol. 24, no. 22, pp. 1549–1551, Nov. 1999, doi: 10.1364/ol.24.001549.

[14] K. Kajihara, Y. Ikuta, M. Oto, M. Hirano, L. Skuja, and H. Hosono, "UV–VUV laser induced phenomena in SiO_2 glass," *Nucl. Instrum. Methods Phys. Res. Sect. B, Beam Interact. Mater. At.*, vol. 218, pp. 323–331, Jun. 2004, doi: 10.1016/j.nimb.2003.12.032.

[15] S. Girard, C. Marcandella, G. Origlio, Y. Ouerdane, A. Boukenter, and J.-P. Meunier, "Radiation-induced defects in fluorine-doped silica-based optical fibers: Influence of a pre-loading with H_2," *J. Non-Crystalline Solids*, vol. 355, nos. 18–21, pp. 1089–1091, Jul. 2009, doi: 10.1016/j.jnoncrysol.2008.11.035.

[16] H. Hosono, M. Mizuguchi, H. Kawazoe, and T. Ogawa, "Effects of fluorine dimer excimer laser radiation on the optical transmission and defect formation of various types of synthetic SiO_2 glasses," *Appl. Phys. Lett.*, vol. 74, no. 19, pp. 2755–2757, May 1999, doi: 10.1063/1.124004.

[17] T. Wijnands, L. K. D. Jonge, J. Kuhnhenn, S. K. Hoeffgen, and U. Weinand, "Optical absorption in commercial single mode optical fibers in a high energy physics radiation field," *IEEE Trans. Nucl. Sci.*, vol. 55, no. 4, pp. 2216–2222, Aug. 2008, doi: 10.1109/TNS.2008.2001859.

[18] E. Guillermain, J. Kuhnhenn, D. Ricci, and U. Weinand, "Macro-bending influence on radiation induced attenuation measurement in optical fibres," *IEEE Trans. Nucl. Sci.*, vol. 61, no. 4, pp. 1834–1837, Aug. 2014, doi: 10.1109/TNS.2014.2306992.

[19] J. Kuhnhenn, S. K. Hoffgen, and U. Weinand, "Quality assurance for irradiation tests of optical fibers: Uncertainty and reproducibility," *IEEE Trans. Nucl. Sci.*, vol. 56, no. 4, pp. 2160–2166, Aug. 2009, doi: 10.1109/TNS.2009.2019605.

[20] E. J. Friebele, C. G. Askins, and M. E. Gingerich, "Effect of low dose rate irradiation on doped silica core optical fibers," *Appl. Opt.*, vol. 23, no. 23, pp. 4202–4208, Dec. 1984, doi: 10.1364/AO.23.004202.

[21] K. Sanada, N. Shamoto, and K. Inada, "Radiation resistance of fluorine-doped silica-core fibers," *J. Non-Crystalline Solids*, vol. 179, pp. 339–344, Nov. 1994, doi: 10.1016/0022-3093(94)90714-5.

[22] E. Guillermain, K. Aikawa, J. Kuhnhenn, D. Ricci, and U. Weinand, "Large-scale procurement of radiation resistant single-mode optical fibers for CERN," *J. Lightw. Technol.*, vol. 33, no. 23, pp. 4878–4884, Dec. 1, 2015, doi: 10.1109/JLT.2015.2449263.

[23] L. Skuja, "Optical properties of defects in silica," in *Defects in SiO_2 and Related Dielectrics: Science and Technology*. Dordrecht, The Netherlands: Springer, 2000, pp. 73–116, doi: 10.1007/978-94-010-0944-7_3.

[24] D. L. Griscom, E. J. Friebele, K. J. Long, and J. W. Fleming, "Fundamental defect centers in glass: Electron spin resonance and optical absorption studies of irradiated phosphorus-doped silica glass and optical fibers," *J. Appl. Phys.*, vol. 54, no. 7, pp. 3743–3762, Jul. 1983, doi: 10.1063/1.332591.

[25] A. Presland, T. Sugito, T. Wijnands, and L. D. Jonge, "Radiation damage to doped Si Fibres in the LHC tunnel," CERN, Geneva, Switzerland, Tech. Rep. LHC-Project-Note-351, Aug. 2004.

[26] A. Billat, J. Blanc, J. Kuhnhenn, and D. Ricci, "Photobleaching effects in multi-mode radiation resistant optical fibers," in *Proc. 17th Eur. Conf. Radiat. Effects Compon. Syst. (RADECS)*, Geneva, Switzerland, Oct. 2017, pp. 53–55, doi: 10.1109/RADECS.2017.8696251.

[27] L. Cognolato, "Chemical vapour deposition for optical fibre technology," *J. Phys. IV*, vol. 5, no. 5, pp. 975–987, Jun. 1995, doi: 10.1051/jphyscol:19955115.

[28] P. Geittner, D. Küppers, and H. Lydtin, "Low-loss optical fibers prepared by plasma-activated chemical vapor deposition (CVD)," *Appl. Phys. Lett.*, vol. 28, no. 11, pp. 645–646, Jun. 1976, doi: 10.1063/1.88608.

[29] D. L. Griscom and E. J. Friebele, "Fundamental radiation-induced defect centers in synthetic fused silicas: Atomic chlorine, delocalized E' centers, and a triplet state," *Phys. Rev. B, Condens. Matter*, vol. 34, no. 11, pp. 7524–7533, Dec. 1986, doi: 10.1103/physrevb.34.7524.

[30] E. M. Dianov *et al.*, "Fluorine-doped silica optical fibres fabricated using plasma chemical technologies," *Proc. SPIE*, vol. 2425, pp. 53–57, Dec. 1994, doi: 10.1117/12.198641.

[31] W. Lieber, X. S. Yi, N. Nontasut, and D. Curticapean, "Differential mode delay (DMD) in graded-index multimode fiber: Effect of DMD on bandwidth tuned by restricted launch conditions," *Appl. Phys. B, Lasers Opt.*, vol. 75, nos. 4–5, pp. 487–491, Oct. 2002, doi: 10.1007/s00340-002-1013-6.

[32] R. Pimpinella and A. Brunsting, "Differential mode delay (DMD) for multimode fiber types and its relationship to measured performance," in *Proc. NFOEC*, Anaheim, CA, USA, Mar. 2005, paper NWF2. [Online]. Available: https://www.osapublishing.org/abstract.cfm?uri=NFOEC-2005-NWF2